DOI: https://doi.org/10.15407/techned2018.04.041

OPTIMAL COUPLING COEFFICIENT CALCULATION FOR INDUCTANCES IN INTERLEAVED BIDIRECTIONAL DC-DC CONVERTERS

K. Tytelmaier[1]*, O. Husev[2], O. Veligorskyi [2]***, M. Khomenko[2]****, D. Maladyka[2]**
[1] Tallinn University of Technology,
st. Ehitajate, 5, Tallinn, 19086, Estonia.
[2] Chernihiv National University of Technology,
st. Shevchenko, 95, Chernihiv, 14035, Ukraine.
e-mail: kostya.tytelmaier@gmail.com, oleksandr.husev@ieee.org, oleksandr.veligorskyi@inel.stu.cn.ua

This paper shows generalized calculation of coupling coefficient for two-phase interleaved bidirectional converter. Switching period of such system was divided on modes and main parameters of the system was analyzed in each mode. Current ripple in each phase can be easily determined using calculation results and it depends on the values of duty cycle and coupling coefficient. It is demonstrated that coupling coefficient affects on current ripple in phase, but not on output current ripple. Based on increasing of the one phase inductance due to coupling an optimal coupling coefficient can be selected. Experimental prototype of bidirectional interleaved two-phase converter proved theoretical hypothesis.
References 15, figures 4.
***Key words**:* bidirectional power flow, circuit analysis, dc-dc power converter, coupling inductors, pulse width modulation converter.

IntroductionMany applications in modern power electronics need high current output, light weight, compact or high overall efficiency of the voltage regulation system. Using just a single phase dc-dc converter sometimes can be limited because of high power dissipation on power semiconductor switches. The main solution for this problem is using of multi-phase or interleaved circuits. That type of converter is widely used in all areas such as powering of different computer systems (such known as VRM or PoL applications), automotive systems, converters for renewable energy systems (as bidirectional power bus between two or more dc voltage busses), PFC schemes, inverters [1, 2, 11]. The main advantages of interleaved converters are high efficiency and power density, better heat dissipation and as a result lower thermal stress on the components. At the same time, drawbacks are increased number of the components (proportionally to number of phases) which result in higher cost and more complicated control algorithm [3-10, 13].

A common practice to decrease the size and weight in interleaved topologies is increasing of switching frequency along with using combined magnetic components also known as a coupled inductors (Fig. 1a). It provides increasing of system integration, power density and also decrease conduction losses or increase the transient response of the system [1]-[10]. Also, it helps redusing phase ripple due to ripple cancelation phenomena, but maximum effect can be achieved when duty cycle is close to *D/N,* where *N* is a number of phases.

Objectives of the paper. The main goal of the paper is representing the method for calculation optimal coupling coefficient in two-phase interleaved bidirectional topology that provide minimal inductor current ripple. The proposed solution can be used for any number of phases as well as unidirectional converters. The analyzed system represented in Fig. 1, *a*.

The main part of the paper. Fig. 1 shows a two-phase interleaved bidirectional converter using an inverse coupled inductor. The coupled inductor can be replaced with leakage inductances L_{lk1} and L_{lk2}, an ideal transformer along with single magnetizing inductance L_m. This model can be called “physical model” since each and every element closely corresponds to the physical structure. The ideal transformer has 1:1 turn’s ratio. The gapping configuration and gap length of inductor affect the value of L_{lk1} and L_{lk2} (which are equal by symmetry $L_{lk1} = L_{lk2} = L_{lk}$, and $L_1 = L_2 = L_s$) and L_m. The relationship between L_{lk}, L_m and L_s (from the general coupled inductor theory) is following

$$L_s = L_m + L_{lk}, \qquad k = L_m (L_{lk} + L_m)^{-1}. \tag{1, 2}$$

ORCID: * http://orcid.org/0000-0001-7582-0204 , ** http://orcid.org/0000-0001-7810-457X ,
*** http://orcid.org/0000-0002-8256-7339 , **** http://orcid.org/0000-0001-9084-3527

It should be noted, that transformer connected with the polarity dots on the opposite ends. Therefore,

$$i_{L_m} = i_{L_1} - i_{L_2} \tag{3}$$

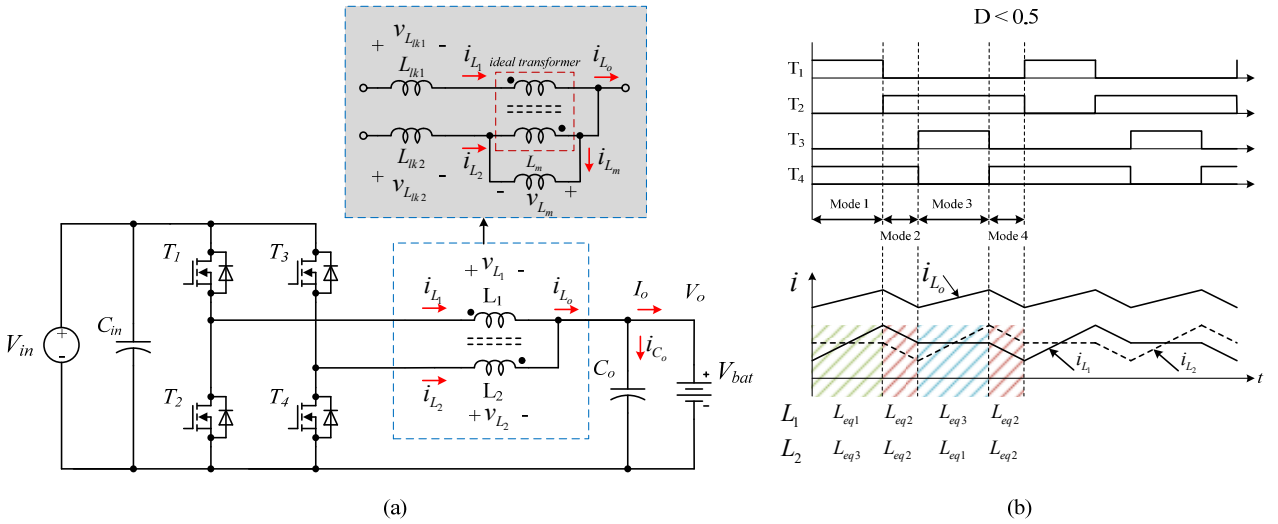

Fig. 1

According to the well-known basic circuit theory, voltages $v_{L_1}, v_{L_2}, v_{L_m}$ can be expressed as

$$v_{L_1} = v_{L_{lk1}} + v_{L_m}, \qquad v_{L_2} = v_{L_{lk2}} - v_{L_m}; \tag{4, 5}$$

$$v_{L_m} = L_m \frac{di_{L_m}}{dt} = L_m \frac{d\left(i_{L_1} - i_{L_2}\right)}{dt}. \tag{6}$$

It can be seen from Fig. 1, *b* that switching period can be divided into four different modes.

Mode 1 [*0 ~ DT*$_s$]. In this mode switches T_1 and, T_4 is turned on, and switches T_2, T_3 are off. The voltage across inductances can be expressed as

$$v_{L_1} = V_{in} - V_o, v_{L_2} = -V_o. \tag{7}$$

From (4, 5), and (7) leakage inductances voltages $v_{L_{lk1}}$ and $v_{L_{lk2}}$ are

$$v_{Llk1} = L_{lk1} \frac{diL_1}{dt} = v_{L_1} - v_{L_m}, \qquad v_{Llk2} = L_{lk2} \frac{diL_2}{dt} = v_{L_2} + v_{L_m}. \tag{8,9}$$

Assuming that $L_{lk1} = L_{lk2} = L_{lk}$ and substitute (8, 9) into (6), the equation for magnetizing inductance voltage v_{L_m} is derived as

$$v_{L_m} = \frac{L_m(v_{L_1} - v_{L_m} - v_{L_2} - v_{L_m})}{L_{lk}}, \qquad v_{L_m} = \frac{L_m(v_{L_1} - v_{L_2})}{L_{lk} + 2L_m}. \tag{10, 11}$$

By substituting (11) back into (8, 9), the inductors currents in mode 1 are

$$\frac{di_{L_1}}{dt} = \frac{1}{L_{lk}}\left(v_{L_1} - \frac{L_m(v_{L_1} - v_{L_2})}{L_{lk} + 2L_m}\right), \qquad \frac{di_{L_2}}{dt} = \frac{1}{L_{lk}}\left(v_{L_2} + \frac{L_m(v_{L_1} - v_{L_2})}{L_{lk} + 2L_m}\right).$$

Based on a volt-seconds balance of the inductors for each cycle during steady state

$$Dv_{L_1} = -(1-D)v_{L_2}; \tag{12}$$

$$\frac{di_{L_1}}{dt} = v_{L_1} \frac{L_{lk} + L_m - \frac{D}{1-D}L_m}{L_{lk}^2 + 2L_m L_{lk}} = \frac{v_{L_1}}{L_{eq_1}}; \tag{13}$$

$$\frac{di_{L_2}}{dt} = v_{L_2} \frac{L_{lk} + L_m - \frac{1-D}{D}L_m}{L_{lk}^2 + 2L_m L_{lk}} = \frac{v_{L_2}}{L_{eq_3}} \tag{14}$$

From (13), (14) equivalent inductance for L_1 and L_2 respectively, in mode 1

$$L_{eq_1} = \frac{L_{lk}^2 + 2L_m L_{lk}}{L_{lk} + L_m - D(1-D)^{-1} L_m} = Ls \frac{1-k^2}{1-kD(1-D)^{-1}}; \quad (15)$$

$$L_{eq_3} = \frac{L_{lk}^2 + 2L_m L_{lk}}{L_{lk} + L_m - (1-D)D^{-1} L_m} = Ls \frac{1-k^2}{1-k(1-D)D^{-1}}. \quad (16)$$

The output current is the sum of two inductor currents (13), (14) and thus it is expressed as

$$\frac{di_{L_o}}{dt} = \frac{V_o}{L_{lk}} \left(\frac{1-2D}{D} \right). \quad (17)$$

Mode 2 [$DT_s \sim T_s/2$]. In mode 2, switches T_2 and T_4 is turned on, and switches T_1, T_3 turned off. Voltages $v_{L_1} = v_{L_2} = -V_o$, thus

$$v_{L_{lk1}} = L_{lk1} \frac{di_{L_1}}{dt} = v_{L_1} - v_{L_m}; \qquad v_{L_{lk2}} = L_{lk2} \frac{di_{L_2}}{dt} = v_{L_2} + v_{L_m}. \quad (18, 19)$$

Substitute (18) and (19) into (6) zero voltage across magnetizing inductance is obtained $v_{L_m} = 0$. Thus from (18) and (19), the inductor currents in mode 2 are

$$\frac{di_{L_1}}{dt} = \frac{di_{L_2}}{dt} = \frac{v_{L_1}}{L_{lk}} = \frac{v_{L_1}}{L_{eq2}}; \quad (20)$$

$$L_{eq2} = L_s - L_m. \quad (21)$$

The output ripple current expressed as

$$\frac{di_{L_o}}{dt} = -\frac{2V_o}{L_{lk}}. \quad (22)$$

Mode 3 [$T_s/2 \sim (T_s/2 + DT_s)$]. In mode 3, switches T_2 and T_3 is turned on, and switches T_1, T_4 turned off. Mode 3 is similar to mode 1, with the only difference that $v_{L_1} = -V_o$ and $v_{L_2} = V_{in} - V_o$. Using the same methods as it was used in mode 1, the inductors output current ripple in mode 3 are derived as follows:

$$\frac{di_{L_1}}{dt} = v_{L_1} \frac{L_{lk} + L_m - (1-D)D^{-1} L_m}{L_{lk}^2 + 2L_m L_{lk}} = \frac{v_{L_1}}{L_{eq_3}}; \quad (23)$$

$$\frac{di_{L_2}}{dt} = v_{L_2} \frac{L_{lk} + L_m - D(1-D)^{-1} L_m}{L_{lk}^2 + 2L_m L_{lk}} = \frac{v_{L_2}}{L_{eq_1}}. \quad (24)$$

The output current in mode 3 is the same as that in mode 1.

Mode 4 [$(T_s/2 + DT_s) \sim T_s$]. In mode 4, switches T_2, T_4 is turned on and switches T_1, T_3 turned off. Mode 4 is exactly the same as mode 2 because $v_{L_1} = v_{L_2} = -V_o$.

In (13), dt is equal to DT_s in mode 1. Therefore, the inductor and output current ripple is expressed as

$$\Delta i_{L_o} = \frac{V_o}{L_{lk}} (1-2D) T_s. \quad (25)$$

From (25) and Fig. 1, it can be seen that the coupling coefficient k does not affect the output current ripple. If L_{lk} is equal to the value of the individual inductor L_s in the non-coupled case, the output current ripple in both non-coupled and coupled inductor is the same.

Analyzing modes, it can be seen that the inductor current ripple depends on the values of D and k. As k increased to 1 (full coupling), the two inductor currents become equal in phase. Thus, the coupling coefficient k has a significant effect on the inductor current ripples although it does not affect the output current ripple.

Current ripple in each phase depends on the equivalent inductance. Plotting results of L_{eq1}/L_s for a range of values for D, it is seen that particular care needs to be taken in choosing k for applications (Fig. 2). Thus current ripple in buck (charge) mode in case of $D < 0.5$

$$\frac{L_{eq1}}{L_s} = \frac{1-k^2}{1-kD(1-D)^{-1}}. \quad (26)$$

Taking into account symmetry of the system, corresponding inductor current ripple in case of $D < 0.5$

$$\frac{L_{eq1}}{L_s} = \frac{1-k^2}{1-k(1-D)D^{-1}}. \qquad (27)$$

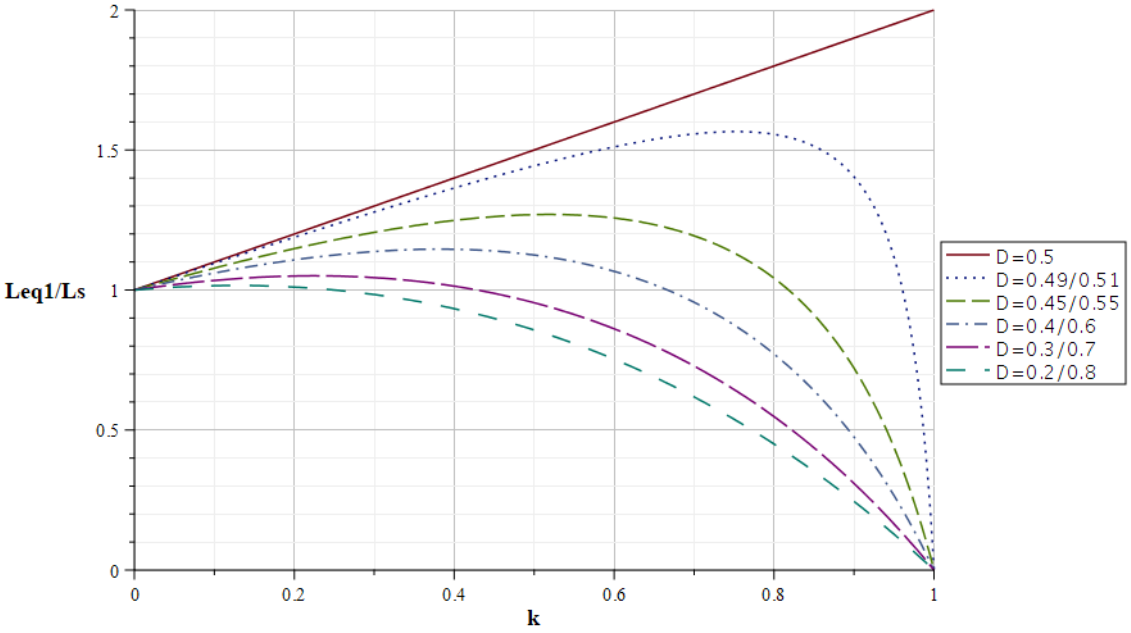

Fig. 2

In boost (discharge) mode equations (27), (26) represent cases for $D > 0.5$ and $D < 0.5$ respectively. For the fixed values of input and output voltages function local extremum (maximum) can be found to achieve the most accurate and optimal coupling coefficient. The represented method can be extended and used for a converter with any even number of phases. For odd number of phases this method should be further improved and recalculated.

Experimental prototype. To verify proposed calculation method, an experimental prototype of two-phase interleaved bidirectional converter with inverse coupled inductors was used (Fig. 3a). Inverse coupling used because of the absence of necessity in high transient response of the system, but need of small conduction losses due to lack of heatsinks.

Parameter	Value
Input voltage, V_{IN}	*4..7.2 V*
Output voltage, V_O	*12 V*
Maximum input current, I_{IN}	*15A*
Maximum output power, P_{Omax}	*100 W*
Switching frequency, f_{SW}	*500 kHz*
Magnetic inductance, L_S	*350 nH*
Coupling coefficient,	*-0.4*
Input/output capacitors, C_{IN}/C_O	*110 µF*

All system parameters represented in the table. Converter works on frequency about 500kHz and based on wide bandgap semiconductor GaN switches (GS61008 from GaN Systems). Input voltage range corresponds to maximum and minimum voltages of two series connected $LiFePO_4$ battery cells from A123 Systems. Based on the possible range of input voltages from the batteries (it can be swing from 4.0 V to 7.2 V for two batteries, which mean D = 0.33…0.6) and taking into account manufacturer accuracy of roughly 10 %, coupling coefficient -0.4 is selected (Fig. 3b). One phase inductance is calculated to achieve Boundary Conduction Mode (BCM) during max load operation [14], [15].

The experimental result shows good performance of the converter in all load range with a maximum efficiency of 96 %. Efficiency was measured using Yokogawa WT1800 precision power analyzer. Waveforms of transistor drain-source voltage and one phase current (Fig. 4) showed very good correlation with theoretically claimed (Fig. 1b) and was measured using Tektronix MSO4043B oscilloscope (bandwidth range 350 MHz) and current probe Tektronix TCP0030A (bandwidth range 100MHz). As a result of right component calculation and selection, the maximum temperature of the inductor, during the long run test with a maximum load of 100 W, is 48.3 °C. Thermal image of the inductor (Fig. 3 c), measured by thermal-imaging camera Fluke Ti10.

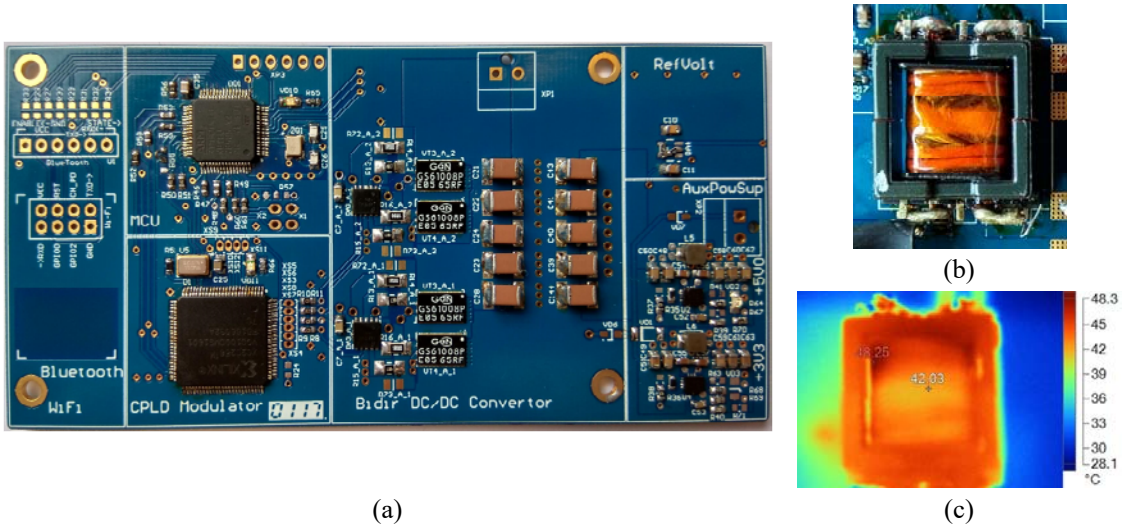

(a) (b) (c)

Fig. 3

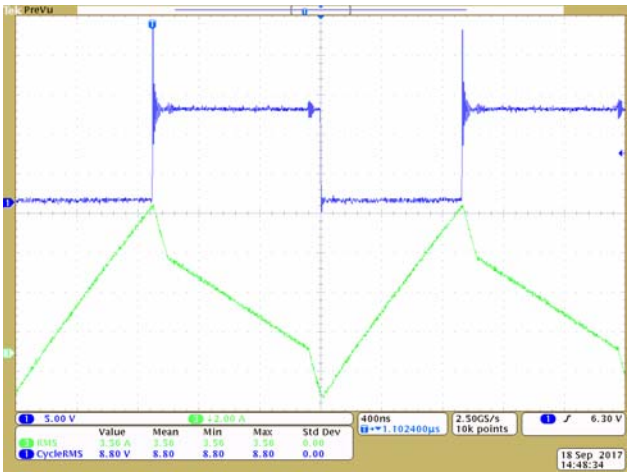

Fig. 4

Conclusions. This paper presents the calculation method for coupling coefficient in bidirectional two-phase interleaved converter. The analytic expression for current ripple during each mode is derived. The coupling can influence only on phase current ripple but not on output current ripple. The overall result of relative equivalent inductance represented in dependency on coupling coefficient showed that for each system it should be chosen optimal coefficient based on working duty cycles. The example experimental design proved calculation approach and that coupled inductors can increase power density and decrease conduction losses in the converters.

Acknowledgment. This research work was supported by Ukrainian Ministry of Education and Science (Grant №0116U004695).

1. Tytelmaier K., Husev O., Veligorskyi O., Yershov R., A Review of Non-Isolated Bidirectional DC-DC Converters for Energy Storage Systems. Proc. of II International Young Scientists Forum on *Applied Physics and Engineering*. Kharkiv, 10-14 October 2016. Pp. 1-7.

2. Wong P.-L., Xu P., Yang B., Lee F.C. Performance Improvements of Interleaving VRMs with Coupling Inductors. *IEEE Transactions on Power Electronics*. 2001. Vol. 16. No. 4. Pp. 499-507.

3. Zu G., McDonald B.A., Wang K. Modeling and Analysis of Coupled Inductors in Power Converters. *IEEE Transactions on Power Electronics*. 2011. Vol. 26. No. 5. Pp. 1355-1363.

4. Shin H.-B., Park J.G., Chung S.-K., Lee H.-W., Lipo T.A. Generalised steady-state analysis of multiphase interleaved boost converter with coupled inductors. *IEE Proc.-Electric Power Application*. 2005. Vol. 152. No. 3. Pp. 584-594.

5. Yang F., Ruan X., Yang Y., Ye Z. Interleaved Critical Current Mode Boost PFC Converter with Coupled Inductor. *IEEE Transaction on Power Electronics*. 2011. Vol. 26. No. 9. Pp. 2404-2413.

6. B. Hesterman. Analysis and Modeling of Magnetic Coupling. *Denver Chapter IEEE Power Electronics Society*. – 2007. – 93 p.

7. Qiu Y. Coupled inductors for power supplies. *EE Times-India*. 2007. Vol. 1. Pp. 1-4.

8. K. Kroics, U. Sirmelis, V. Brazis. Design of coupled inductor for interleaved boost converter. *Przeglad Elektrotechniczny*. 2014. Vol. 12. Pp. 91-94.

9. Ayele G.T. Challenges of Multi-channel Interleaved Bidirectional Power Converters and their Digital Solutions: author`s abstract of Dr. tech. sci. diss. University of Nottinghan. Nottinghan. 2015. 73 p.

10. Ikriannikov A. The benefits of the coupled inductor technology. *Maxim Integrated tutorial 5997*. – 2014. – 10 p.

11. Yao K. High Frequency and High-Performance VRM Design for the Next Generation of Processors: author`s abstract of Dr. tech. sci. diss. Virginia Polytechnic Institute and State University. Blacksburg. 2004. 193 p.

12. Wong P.-L., Performance Improvement of Multi-Channel Interleaved Voltage Regulator Modules with Integrated Coupling Inductors: author`s abstract of Dr. tech. sci. diss. Virginia Polytechnic Institute and State University. Blacksburg. 2001. 224 p.
13. Mu M., Lee F.C., Jiao Y., Lu S. Analysis and Design of Coupled Inductor for Interleaved Multiphase Three-Level DC-DC Converter. *Applied Power Electronica Conference and Exposition (APEC)*. Charlotte. 15-19 March 2015. Pp. 2999-3006.
14. *Texas Instruments.* SLVA477B Basic calculation of a Buck Converters Power Stage. – 2015. – 8 p.
15. *Texas Instruments*. AN-1197 Selecting Inductors for Buck Converter. – 2013. – 18 p.

УДК 621.316.721

РАСЧЕТ ОПТИМАЛЬНОГО КОЭФФИЦИЕНТА МАГНИТНОЙ СВЯЗИ ИНДУКТИВНОСТЕЙ В ДВУНАПРАВЛЕННОМ ПРЕОБРАЗОВАТЕЛЕ ПОСТОЯННОГО ТОКА С ЧЕРЕДУЮЩИМИСЯ ФАЗАМИ

К. Тительмаер[1], А. Гусев[2], А. Велигорский[2], М. Хоменко[2], Д. Маладыка[2]
[1] Таллинский Технологический Университет,
ул. Эхитаджате, 5, Таллинн, 19086, Эстония.
[2] Черниговский Национальный Технологический Университет,
ул. Шевченка, 95, Чернигов, 14035, Украина.
e-mail: kostya.tytelmaier@gmail.com, oleksandr.husev@ieee.org, oleksandr.veligorskyi@inel.stu.cn.ua

Представлен обобщенный расчет коэффициента магнитосвязанности для двухфазного двунаправленного преобразователя с чередующимися фазами. Период переключения такой системы был разделен на режимы, и основные параметры системы были проанализированы в каждом из режимов. Пульсации тока в каждой фазе могут быть легко определены с использованием результатов расчета и зависят от значений скважности и коэффициента связи. Также было показано, что коэффициент магнитной связи влияет на пульсации тока в фазе, но не на пульсации выходного тока. Исходя из увеличения индуктивности одной фазы за счет магнитной связи, было выбрано оптимальное значение коэффициента магнитной связи. Экспетиментальный прототип двунаправленного двухфазного преобразователя с чередующимися фазами подтвердил правильность методики расчета коэффициента магнитной связи. Библ. 15, рис. 4.

Ключевые слова: двонаправленый поток энергии, анализ схемы, преобразователь постоянного тока, магнитосвязанные индуктивности, преобразователи с широтно-импульсною модуляцией.

УДК 621.316.721

РОЗРАХУНОК ОПТИМАЛЬНОГО КОЕФІЦІЄНТА МАГНІТОЗЧЕПЛЕННЯ ІНДУКТИВНОСТЕЙ В ДВОНАПРАВЛЕНОМУ ПЕРЕТВОРЮВАЧІ ПОСТІЙНОГО СТРУМУ З ЧЕРЕДУВАННЯМ ФАЗ

К. Тительмаєр[1], О. Гусев[2], О. Велігорський[2], М. Хоменко[2], Д. Маладика[2]
[1] Талліннський Технологічний Університет,
вул. Ехітаджате, 5, Таллінн, 19086, Естонія.
[2] Чернігівський Національний Технологічний Університет,
вул. Шевченка, 95, Чернігів, 14035, Україна.
e-mail: kostya.tytelmaier@gmail.com, oleksandr.husev@ieee.org, oleksandr.veligorskyi@inel.stu.cn.ua

Показано узагальнений розрахунок коефіцієнта магнітозчеплення для двофазного двонаправленого перетворювача з чередуванням фаз. Період перемикання такої системи був поділений на режими, основні параметри системи були проаналізовані в кожному режимі. Пульсації струму в кожній фазі можуть бути легко визначені з використанням результатів розрахунку, і вони залежать від значень шпаруватості та коефіцієнта зчеплення. Також було показано, що коефіцієнт магнітозчеплення впливає на пульсації струму в фазі, але не впливає на пульсації вихідного струму. Виходячи зі збільшення індуктивності однієї фази за рахунок магнітозв`язку, було обрано оптимальний коефіцієнт зчеплення. Експериментальний прототип двонаправленого двофазного перетворювача з чередуванням фаз підтвердив правильність методики розрахунку коефіцієнта магнітозчеплення. Бібл. 15, рис. 4.

Ключові слова: двонаправлений потік енергії, аналіз схеми, перетворювач постійного струму, магнітозв`язані індуктивності, перетворювачі з широтно-імпульсною модуляцією.

Надійшла 07.02.2018
Остаточний варіант 13.03.2018